Rare Metal Materials and Engineering
Volume 51, Issue 11, November 2022
Available online at www.rmme.ac.cn

Science Press

Cite this article as: An Dongyang, Liu Chenfei, Zhao Shuang, et al. High-Temperature Thermal Shock Performance of Si-Ti-Cr Silicide Coating on Nb-Hf Alloy Surface in Atmosphere and Vacuum[J]. Rare Metal Materials and Engineering, 2022, 51(11): 3974-3980.

ARTICLE

High-Temperature Thermal Shock Performance of Si-Ti-Cr Silicide Coating on Nb-Hf Alloy Surface in Atmosphere and Vacuum

An Dongyang[1,2], Liu Chenfei[1], Zhao Shuang[1], Zhang Haipeng[3], Tang Zengwu[1], Xiao Peng[2], Dai Jingmin[2], Wang Yaming[3]

[1] Beijing Xinghang Mechanical-Electrical Equipment Co., Ltd, Beijing 100074, China; [2] School of Instrumentation Science and Engineering, Harbin Institute of Technology, Harbin 150001, China; [3] Institute for Advanced Ceramics, Harbin Institute of Technology, Harbin 150001, China

Abstract: To improve the high-temperature thermal shock performance, the Si-Ti-Cr silicide coatings were prepared on Nb-Hf alloy by slurry sintering and high-temperature permeation methods. The high-temperature thermal shock performance of Si-Ti-Cr silicide-coated Nb-Hf alloys in atmosphere and vacuum was comparatively analyzed. The failure mechanism of Si-Ti-Cr coating in atmosphere and vacuum after thermal shock tests was determined by simulating the temperature and thermal stress distributions of the coating during thermal shock. Results show that the mass loss of the coating in vacuum is less than 0.8 mg/cm^2 after 100 thermal shock cycles at 1300 °C. The mass gain of the coating in atmosphere is less than 3 mg/cm^2 after 200 thermal shock cycles at 1600 °C. Therefore, the silicide coating exhibits excellent thermal shock resistance at 1300 °C in vacuum and at 1600 °C in atmosphere.

Key words: silicide coating; thermal shock performance; thermal stress distribution; failure mechanism

Liquid rocket engines, particularly the two-component engines, are commonly used for orbit control of spacecrafts[1-4], and their maximum operation temperature can reach over 2700 °C in the combustor section of the thrust chamber. Although the injector, mixing ratio, and coating cooling are optimized to reduce the temperature, the wall temperature of the combustor section is usually higher than 1000 °C[5]. The traditional structural materials can hardly meet the dual requirements of high temperature performance and oxidation resistance[6-8]. It is reported that the surface coating of materials has both the excellent high temperature mechanical properties and the high temperature oxidation resistance[9-13].

With the improvement of the propellant ratio and reliability of engines, the thermal protective coatings are more and more important for oxidation resistance enhancement of Nb alloy components in aerospace[14-16]. The thermal protective coatings can endure the complex and extremely harsh environment under the high-temperature multi-field coupled mode. Therefore, the high-temperature mechanical properties, thermal shock resistance, and failure mechanism of the thermal protective coating on high-temperature metals should be investigated[17-19]. It is known that the thermal shock is the major contributor for the coating failure[20-22]. Because the coated Nb alloy components will serve in various environments, including the atmosphere and vacuum[23], the thermal shock resistance of coated Nb alloy in atmosphere and vacuum should be both considered.

Therefore, to improve the thermal shock resistance of the silicide coatings, the Si-Ti-Cr silicide coatings were prepared on Nb-Hf alloy by slurry sintering and high-temperature permeation methods in this research. The high-temperature thermal shock resistance of Si-Ti-Cr silicide coated Nb-Hf alloys in atmosphere and vacuum was comparatively analyzed. The failure mechanism of coating under thermal shock cycles was analyzed by the three-

---

Received date: February 27, 2022
Foundation item: National Defense Technical Basic Research Program of China (JSZL 2015603 B 002); Aviation Science Fund Project (20172777007); National Basic Science Research Program (52206225)

Corresponding author: An Dongyang, Ph. D., Beijing Xinghang Mechanical-Electrical Equipment Co., Ltd, Beijing 100074, P. R. China, E-mail: zdady1989@163.com

dimensional heat transfer modeling and the simulated thermal stress distribution.

1 Experiment

The Nb-Hf alloy was coated by slurry spraying method. The vacuum melting was used to melt or semi-melt the mixture powder. During the vacuum melting, different functional substances in the diffusion transition layer and dense layer were formed by the reaction and diffusion of elements in the melt, such as Ti and Si. Finally, when the melt cooled down and hardened, the coating was formed. The outer layer of the coating was mainly composed of complex (Nb, Cr, Ti)Si_2 phases. The diffusion transition layer was composed of the dense mixed phases of (Nb, Ti)Si_2 and $(Nb, Ti)_5Si_3$. With further exposing the coating in air at high temperatures (>1300 °C), the $(Nb, Cr, Ti, Si)_xO_y$ compound was formed through the oxidation, impeding the oxygen diffusion to the coating interface and substrate and thereby enhancing the oxidation resistance of the coating.

The specimens with the size of 70 mm×10 mm×1 mm were cut from the NbHf 10-1 alloy raw plate. The specimen edge was polished by sandpaper, and the surface was cleaned by acetone and then dried. Then the specimen was acid-washed for the preparation of the silicide coating. The purity of silica, titanium, and chromium powders is all above 99.9%, and the average particle size is around 2 μm. The methacrylate-copper and polyvinyl butyral were used as solvent and binder, respectively. The slurry was prepared with the powder ratio of Si:Cr:Ti=8:1:1. Afterwards, the functional elements with different contents, 10wt% binder, and solvents were added. The slurry was coated evenly on the specimen surface by spraying. Finally, the specimen was placed in the vacuum sintering furnace at 1400~1500 °C for 10~30 min, and the Si-Cr-Ti silicide coating with thickness of 100 μm was obtained.

The basic phase and microstructure of the coatings were characterized by X-ray diffraction (XRD, Empyrean, Panalytical, Netherlands) with Cu Kα radiation at 30 mA and 40 kV. The scanning electron microscope (SEM, Quanta 200 FEG, USA) coupled with energy disperse spectroscope (EDS) was used to analyze the surface and cross-section of the coatings.

The experiment device is shown in Fig.1, including a high-temperature thermal shock test bench, copper cylinders, and an optical fiber pyrometer with the accuracy of 0.001 °C. The coated specimen (70 mm×10 mm×1 mm) was heated to the required temperatures (1000, 1100, 1200, and 1300 °C in vacuum; 1300, 1450, and 1600 °C in air) in ~10 s, and then air-cooled to 500 °C. The infrared temperature measurement system was employed.

The thermal shock cycle life of the coatings was measured. The surface condition of the coating was checked during the heating process and after the tests to insure the inexistence of black oxidation marks with the diameter of >2 mm or large drop failure of the coating.

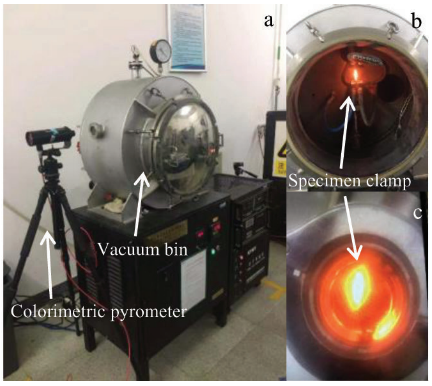

Fig.1 Appearances of thermal shock resistance experiments in vacuum and air: (a) experiment device; (b) thermal shock experiment in air; (c) thermal shock experiment in vacuum

2 Results and Discussion

2.1 XRD analysis

As shown in Fig. 2, XRD patterns show that $NbSi_2$ and Nb_5Si_3 are the main phases of the specimens after 100 thermal shock cycles at 1000, 1100, 1200, and 1300 °C in vacuum. Besides, a small amount of $TiSi_2$ is found, which is consistent with the phase of the matrix coating. Under the vacuum condition, no oxygen is diffused into the coating, i. e., no oxidation phase is formed. Because the thermal shock temperature is lower than the sintering temperature, the driving force is insufficient for the element diffusion in the coatings. Therefore, the phases in the coatings remain.

Fig. 3 shows XRD patterns of the specimens after 200 thermal shock cycles in air at 1300, 1450, and 1600 °C. The main phases of the coatings after the thermal shock in air are $NbSi_2$, Nb_5Si_3, and SiO_2, and a small amount of Nb_2O_5 is also found in the coatings, which indicates that the oxygen is diffused into the coating during the thermal shock cycles, and it preferentially reacts with the free silicon to form SiO_2. The oxygen can react with $NbSi_2$ to form the SiO_2 and Nb_2O_5, as expressed by Eq.(1)[24], as follows:

$$4NbSi_2+13O_2=8SiO_2+2Nb_2O_5 \tag{1}$$

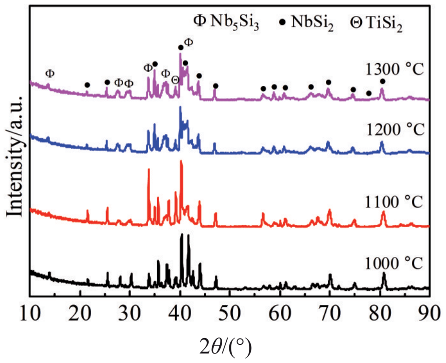

Fig.2 XRD patterns of specimens after 100 thermal shock cycles in vacuum at 1000, 1100, 1200, and 1300 °C

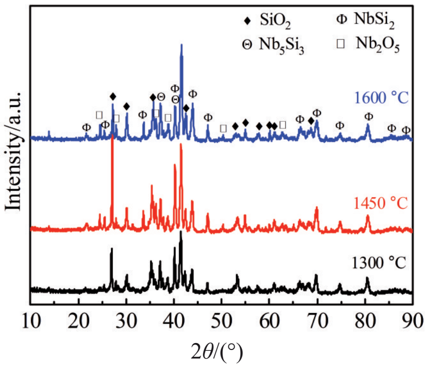

Fig.3 XRD patterns of specimens after 200 thermal shock cycles in air at 1300, 1450, and 1600 °C

2.2 Microstructure and element composition

Fig. 4a and 4b show SEM morphologies of the silicide coating on the NbHf 10-1 alloy. It can be observed that the coating surface is formed by grain sintering. Besides, there are many pores and a few micro-cracks on the surface. However, the pores and micro-cracks only exist in the surface layer, which is caused by the volatilization of the additives during the surface sintering, and the inner layer of the coating is densely bonded. The cross-section morphology shows that the silicide coating has a double-layer structure. EDS analyses show that the point A and point B are basically the Nb_5Si_3 and $NbSi_2$, respectively. Therefore, there is a transition layer (Nb_5Si_3 layer) between the substrate and the external coating ($NbSi_2$ layer)[24].

The double-layer coating is better than the single silicide coating in the oxidation resistance, since the transition layer can still impede the oxygen diffusion when the outer layer ($NbSi_2$ layer) is completely oxidized. Thus, the matrix is well protected. Moreover, it can be observed that the total thickness of the coating is about 106 μm: the transition layer is about 10.9 μm and the outer layer is about 95.1 μm. According to the element ratio at point A (Si:Nb=0.59), the transition layer is composed of the Nb_5Si_3 phase, which is formed by Si diffusion. Because the element ratio at point B is Si:Nb=1.76, the outer layer consists of the $NbSi_2$ phase, which is also formed by diffusion.

Fig. 5 shows the surface morphologies of the coating after thermal shock cycles in vacuum at 1000, 1100, 1200, and 1300 °C. Fewer pores appear on the silicide coating of NbHf 10-1 alloy, compared with Fig.4. With increasing the thermal shock temperature, the surface roughness is decreased, but the cracks are gradually increased with the dendritic diffusion, as indicated by the cycles in Fig.5. The falling off of loose layer is the main reason for the roughness reduction, thereby exposing the dense $NbSi_2$ layer during thermal shock cycles in vacuum. Due to the difference in thermal expansion coefficients of the coating and the substrate, the relatively large thermal stress appears periodically between the coating and the interface and between the coating and the substrate during thermal shock cycles, which leads to the stress fatigue of the coatings. Therefore, a large number of cracks occur on the coating surface. Fig. 6 shows that the cracks form in the $NbSi_2$ layer due to the stress fatigue. It can be seen that the cracks penetrate the coating interface and the substrate. With increasing the temperature, the number and the size of cracks are both increased.

The surface and cross-section morphologies of the coatings after the thermal shock cycles in air are shown in Fig. 7 and Fig.8, respectively. As shown in Fig.7, after 200 thermal shock cycles in air at 1300 °C, the coating surface is loose and the grain bonding is incompact, but no obvious cracks can be observed. When the temperature rises to 1450 °C, the micro-cracks appear on the coating surface, the grain bonding becomes closer, and the surface roughness decreases. With increasing the temperature to 1600 °C, the coating surface becomes smooth and the brittle cracks appear, forming the glaze layer. This is because the silicon dioxide is in the glass state at high temperature (1650 °C). Thus, the silicon dioxide can act as the binder to bond grains to form the compact glass coating, thereby preventing the oxygen diffusion and improving the oxidation resistance of the coating. Therefore, SiO_2 is an important high-temperature resistance in coating. However, the glass-ceramic coating is brittle and prone to crack under the cyclic thermal stress. As shown in Fig.8, some

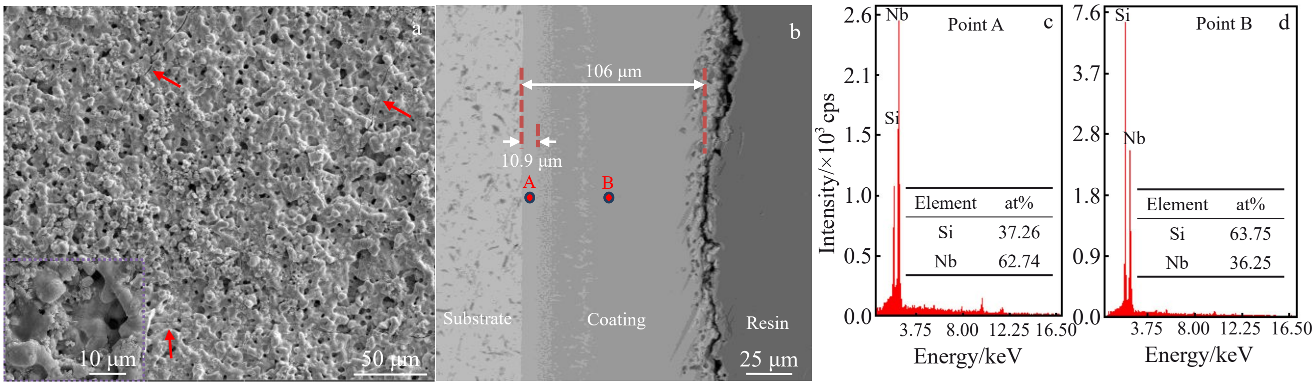

Fig.4 SEM surface morphology (a) and cross-section morphology (b) of the silicide coating on NbHf 10-1 alloy; EDS analyses of point A (c) and point B (d) in Fig.4b

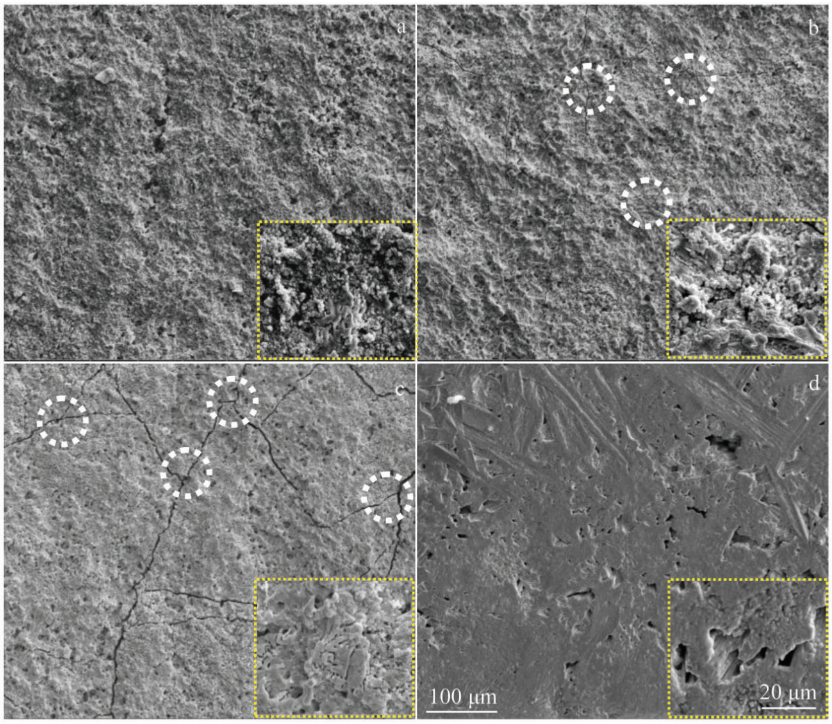

Fig.5 Surface morphologies of coatings after 100 thermal shock cycles in vacuum at 1000 °C (a), 1100 °C (b), 1200 °C (c), and 1300 °C (d)

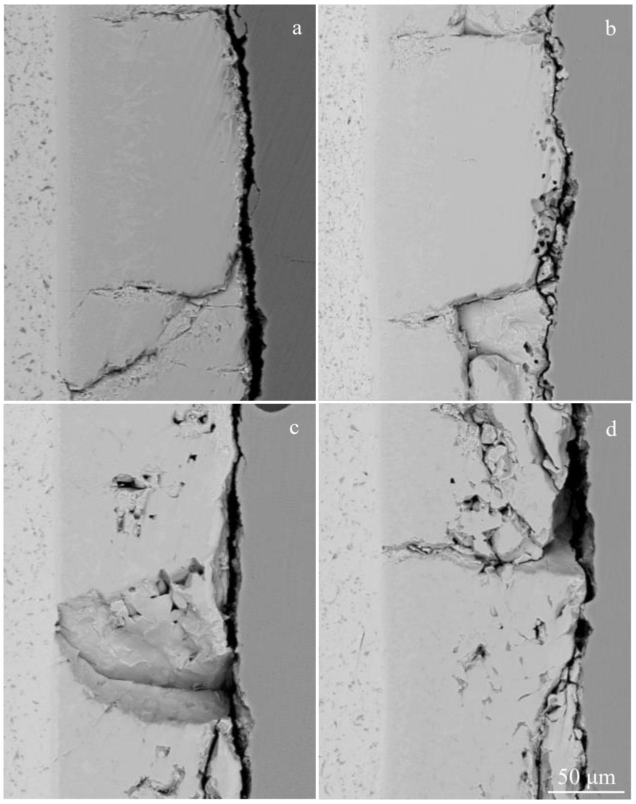

Fig.6 Cross-section morphologies of the silicide coatings after 100 thermal shock cycles in vacuum at 1000 °C (a), 1100 °C (b), 1200 °C (c), and 1300 °C (d)

cracks penetrate the interfaces between the coating and the substrate, undermining the oxidation resistance of the coating to a great extent. In addition, due to the short thermal shock period and oxidation duration, the thickness of the transition layer (Nb_5Si_3) barely changes.

2.3 Mass variation

As shown in Fig. 9, the coating mass gradually decreases during the thermal shock cycles in vacuum, because no element diffusion occurs into the coating. Besides, the coating surface is continuously shed due to the thermal stress. With increasing the thermal shock temperature, the mass loss per unit area of the coating is increased gradually during the thermal shock cycles. After 100 thermal shock cycles in vacuum at 1000 °C, the mass loss of the coating is 0.35 mg/cm^2. In comparison, when the temperature rises to 1300 °C, the mass loss is 0.79 mg/cm^2, which is increased by 126%. The results show that a remarkable increase in thermal stress inside the coating occurs with increasing the temperature, according to the cracking and mass loss of the coating.

The mass gain curves of the coatings after thermal shock cycles in air at 1300, 1450, and 1600 °C are shown in Fig.10. The coating mass continuously increases at 1300 and 1450 °C. In the first 10 cycles, the mass gain of the coating is fast, and then it gradually slows down. During the thermal shock tests at 1300 °C, the mass gain of the coating increases linearly. After 600 thermal shock cycles, the maximum mass gain reaches 3 mg/cm^2, and the mass gain still presents the increasing trend. During the thermal shock test at 1450 °C, the coating mass is increased rapidly in the initial stage. However, after 200 thermal shock cycles, the mass gain increases slowly. After 400 thermal shock cycles, the mass gain reaches 2.9 mg/cm^2, which indicates that the mass gain caused by the coating oxidation mainly occurs in the early stage. When the

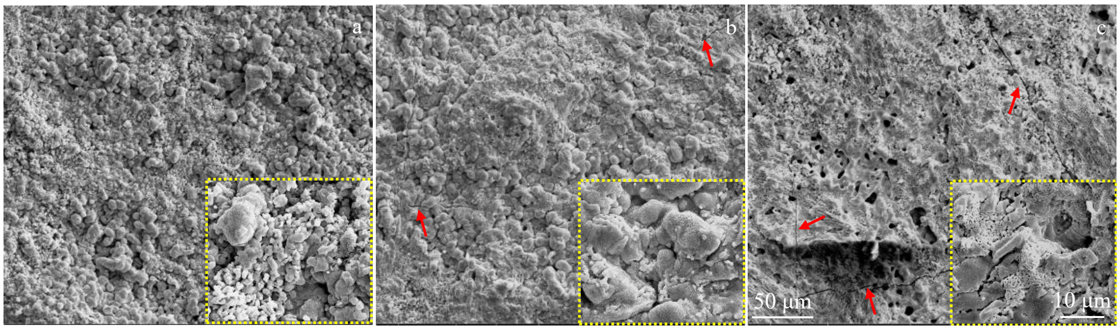

Fig.7 Surface morphologies of the silicide coatings after 200 thermal shock cycles in air at 1300 °C (a), 1450 °C (b), and 1600 °C (c)

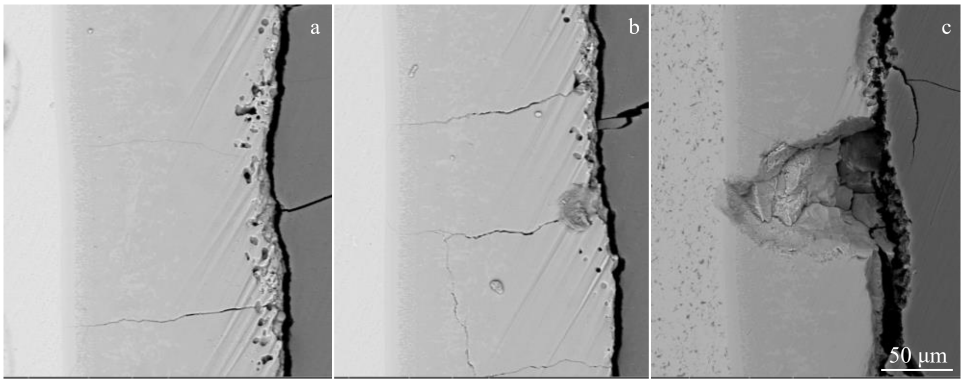

Fig.8 Cross-section morphologies of the silicide coatings after 200 thermal shock cycles in air at 1300 °C (a), 1450 °C (b), and 1600 °C (c)

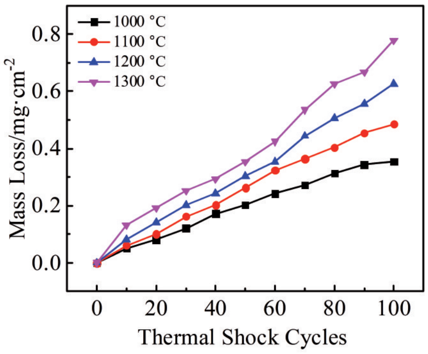

Fig.9 Mass loss of the silicide coatings during thermal shock cycles in vacuum at 1000, 1100, 1200, and 1300 °C

temperature rises to 1600 °C, in the first 15 thermal shock cycles, the mass gain of the coating reaches 1.9 mg/cm^2 rapidly. Afterwards, the coating mass is decreased, which is consistent with the previous results of the surface morphology. A dense SiO_2 glass layer is formed at high temperature, thereby preventing the oxygen diffusion into the interior coating. Moreover, the cracking and shedding of the brittle glass-ceramic coating caused by the thermal stress also lead to the mass loss of coating.

2.4 Simulation of thermal stress distribution

As shown in Fig.11, when the specimen is heated rapidly to 1500 °C within 30 s, the temperature gradually decreases from the middle part to both ends. The maximum temperature in the middle part is 1772.45 K. The gradient distribution of the temperature results in the thermal stress in the coating. The thermal stress in the middle part of the specimen is the

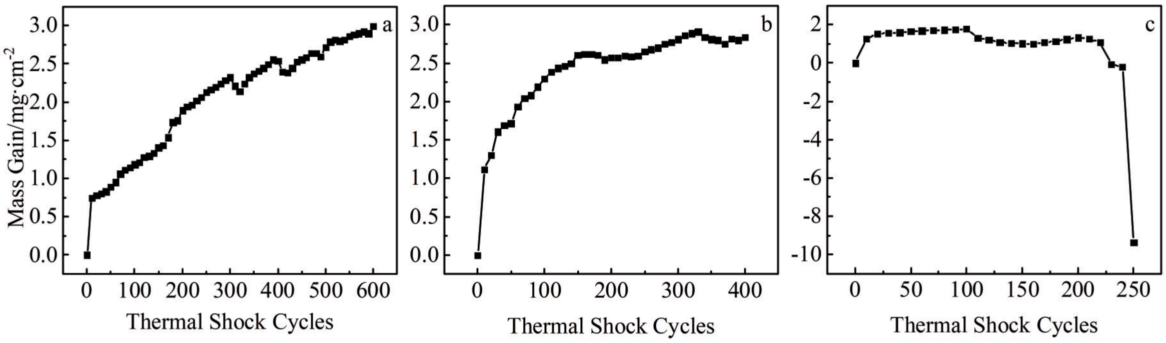

Fig.10 Mass gain of the silicide coatings during thermal shock cycles in air at 1300 °C (a), 1450 °C (b), and 1600 °C (c)

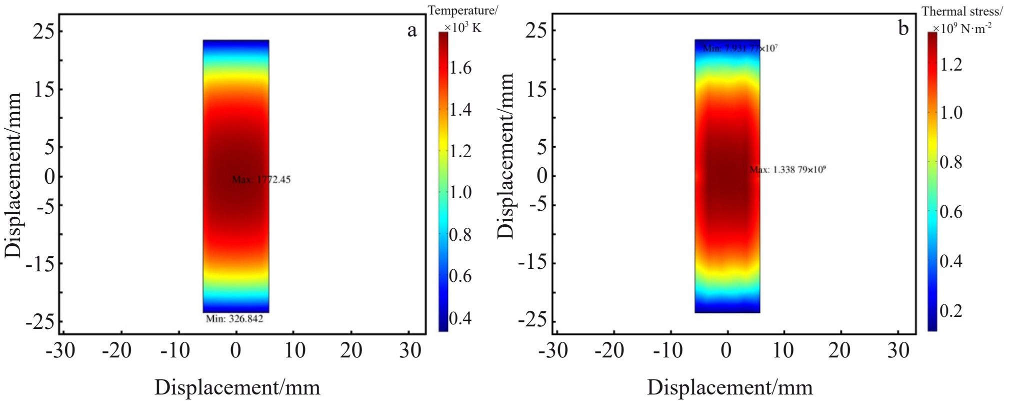

Fig.11 Simulation diagrams of heat distribution of the specimen during heating (a) and thermal stress distribution of the specimen during vacuum thermal shock cycle (b)

strongest of ~1.34×10^9 N/m^2. Therefore, the failure of coatings starts from the middle part. Based on the results in this research, it can be concluded that the maximum working temperature of the coatings is less than 1300 °C in vacuum and less than 1600 °C in air.

3 Conclusions

1) The interface transition layer of Si-Ti-Cr coating is composed of Nb_5Si_3 phase formed by the diffusion of silicon and other elements. The outer layer is composed of $NbSi_2$ phase. The coating is dense, well bonded with the matrix, and has good oxidation resistance.

2) The coating mass loss is caused by the surface shedding. The coating mass is stable during the first 200 thermal shock cycles in air at 1600 °C because of the dense SiO_2 glass layer formed on the coating surface, which prevents the oxygen diffusion into the interior coating. Then the coating gradually fails due to the shedding caused by the strong thermal stress.

3) The maximum working temperature of the coatings is less than 1300 °C in vacuum and less than 1600 °C in air.

References

1 Shelley J S, Leclaire R, Nichols J. *JOM*[J], 2001, 53(4): 18
2 Kim K O, Roh T, Lee J W *et al. Reliability Engineering and System Safety*[J], 2016, 146: 13
3 Bucchi A, Bruno C, Congiunti A. *Journal of Spacecraft and Rockets*[J], 2005, 42(3): 476
4 Gotsulenko V V. *Journal of Engineering Thermophysics*[J], 2008, 81(5): 935
5 Bobzin K, Ernst F, Zwick J *et al. Journal of Thermal Spray Technology*[J], 2008, 17(3): 344
6 Cheng X Y, Yu Y G, Zhang D M *et al. Journal of Thermal Spray Technology*[J], 2020, 29(7): 1804
7 Sakidja R, Park J S, Hamann J *et al. Scripta Materialia*[J], 2005, 53(6): 723
8 Fu Q G, Li H J, Shi X H *et al. Surface and Coatings Technology*[J], 2006, 201(6): 3082
9 Kumar S, Kumar R. *Surface Engineering*[J], 2021, 37(11): 1339
10 Cui Y, Shen J Q, Manladan S M *et al. Applied Surface Science*[J], 2020, 512: 145 736
11 Mitra R. *International Materials Reviews*[J], 2006, 51(1): 13
12 Tang Z H, Thom A J, Kramer M J *et al. Intermetallics*[J], 2008, 16(9): 1125
13 Perepezko J H, Sossaman T A, Taylor M. *Journal of Thermal Spray Technology*[J], 2017, 26(5): 929
14 Chang Y Y, Hsiao C Y. *Surface and Coatings Technology*[J], 2009, 204(6): 992
15 Li X, Guo X P, Qiao Y Q. *Oxidation of Metals*[J], 2015, 83(3): 253
16 Kablov E N, Zhestkov B E, Grashchenkov D V *et al. High Temperature*[J], 2017, 55(6): 873
17 Xie S M, Lin S S, Shi Q *et al. Surface and Coatings Technology*[J], 2021, 413: 127 092
18 Wang Y, Tian W, Yang Y. *Surface and Coatings Technology*[J], 2007, 201(18): 7746
19 Yan Z Q, Feng C, Xiang X J *et al. Journal of Composite Materials*[J], 2010, 44(26): 3085
20 Zhang C, Wang H, Liu Y *et al. Advance in Applied Ceramics*[J], 2014, 112(8): 499
21 Huang W Z, Yu Z, Fan X Z *et al. Journal of Thermal Spray Technology*[J], 2013, 22(6): 918
22 Li W G, Li D Y, Cheng T B *et al. Engineering Fracture Mechanics*[J], 2012, 82: 9
23 Tyagi M, Ghosh S K, Tewari R. *Surface Engineering*[J], 2020, 36(2): 158
24 Ge Y L, Wang Y M, Chen J C H *et al. Journal of Alloys and Compounds*[J], 2018, 767: 7

Nb-Hf合金表面Si-Ti-Cr硅化物涂层在大气和真空中的高温热震性能

安东阳[1,2]，刘晨飞[1]，赵　爽[1]，张海鹏[3]，唐增武[1]，萧　鹏[2]，戴景民[2]，王亚明[3]
(1. 北京星航机电装备有限公司，北京 100074)
(2. 哈尔滨工业大学 仪器科学与工程学院，黑龙江 哈尔滨 150001)
(3. 哈尔滨工业大学 特种陶瓷研究所，黑龙江 哈尔滨 150001)

摘　要：为了提高Nb-Hf合金的高温热震性能，采用浆料烧结和高温渗透法制备了Si-Ti-Cr硅化物涂层，对比分析了Si-Ti-Cr硅化物包覆的Nb-Hf合金样品在大气和真空条件下的高温热震性能。通过模拟在热冲击过程中涂层的温度场和热应力场分布，揭示了Si-Ti-Cr涂层在大气和真空条件下的热冲击失效机理。结果表明，在1300 ℃热震循环100次条件下，涂层的真空失重小于0.8 mg/cm^2；在1600 ℃热震循环200次条件下，涂层的空气增重小于3 mg/cm^2。硅化物涂层在1300 ℃真空环境下和1600 ℃空气环境下具有优异的抗热震性能。

关键词：硅化物涂层；热震性能；热应力分布；失效机理

作者简介：安东阳，男，1989年生，博士，工程师，北京星航机电装备有限公司，北京 100074，E-mail：zdady1989@163.com